RSC Advances

PAPER

View Article Online
View Journal | View Issue

Cite this: *RSC Adv.*, 2022, **12**, 8530

Study on SO_2 and Cl_2 sensor application of 2D PbSe based on first principles calculations

Jiwei Zhang,[a] Jianhua Pang,*[a] Hui Chen,[a] Guang Wei,[a] Songrui Wei,*[b] Jin Yan[a] and Shaowei Jin[c]

In this paper, we use 2D PbSe to design a gas sensor to monitor the presence of SO_2 and Cl_2. We use first principles to verify the feasibility of this material, such as atomic structure, band gap, differential charge density and Bader charge. The results show that 2D PbSe can distinctly adsorb SO_2 and Cl_2. Furthermore, the adsorption of SO_2 and Cl_2 will affect the electronic structure of 2D PbSe, and some electrons in the PbSe are transferred to gas atoms. The band gap of the system after adsorption is smaller than that of the PbSe before adsorption. The band gap of single layer PbSe decreases by 41.92% after SO_2 adsorption and 60.61% after Cl_2 adsorption. The band gap of multi-layer PbSe decreases by 72.97% after SO_2 adsorption and 43.24% after Cl_2 adsorption. This shows that single layer PbSe is more sensitive to Cl_2 and multi-layer PbSe is more sensitive to SO_2. It provides a potential possibility for designing gas sensors for SO_2 and Cl_2 based on 2D PbSe.

Received 24th February 2022
Accepted 10th March 2022

DOI: 10.1039/d2ra01249a

rsc.li/rsc-advances

1. Introduction

Two-dimensional materials are considered as excellent new materials due to their good conductivity, damage resistance, heat shock resistance, ease of processing and other advantages.[1] Many 2D materials show outstanding performance in various fields because of their unique properties, such as enhanced optical transparency, excellent conductivity and outstanding mechanical strength.[2–5] More than 30 MXene materials are synthesized experimentally, and hundreds of possible compositions are predicted theoretically.[6] Among them, some MXene materials are more suitable as gas sensor materials because of their adjustable band gap.[7–9]

Cl_2 is a highly toxic gas with a strong pungent odour, and it can cause great damage to the human respiratory system.[10] SO_2 is a kind of irritant sulfur oxide, one of the main pollutants in the atmosphere, and the major contributor to acid rain. At the same time, it is a kind of carcinogen, and long-term exposure to industrial pollutants containing high levels of SO_2 can increase the risk of cancer.[11] In this context, the effective detection of these harmful gases is useful to protect the environment and human health.[12,13]

PbSe is a binary lead sulfur compound, and this material has performed well in the fields of photoelectric detection, photoluminescence and so on.[14,15] According to the reference, PbSe with rocksalt structures can be prepared as monolayer PbSe by mechanical exfoliation and wet chemical synthesis.[16–21] In this way, its surface area will be greatly increased and it will become more sensitive. At the same time, we find that Wang's report showed that Cl doping caused the decrease of PbSe resistance.[22] Therefore, it is feasible to detect Cl_2 with PbSe.

In this paper, based on first principle calculation, we study the adsorption property of the single layer PbSe material and multi-layer PbSe. We find that the 2D PbSe can adsorb SO_2 and Cl_2. When Cl_2 is adsorbed on PbSe, the bond between Cl atoms breaks. However, for SO_2, the bond does not break. Additionally, we also find electron transfer in the adsorption process. It helps to understand the physical origin of the adsorption process and change of conduction. Based on the change of conduction, we can judge whether the material adsorbs Cl_2 and SO_2. Based on these results, the PbSe is a potential sensor material for monitoring the presence of SO_2 and Cl_2 in the environment.

2. Materials and methods

All calculations are carried out using the density functional theory, implemented in Vienna *Ab Initio* Simulation Package (VASP).[23–25] Due to the large computing system, the exchange–correlation potential is employed by the generalized gradient approximation (GGA) with Perdew–Burke–Ernzerhof (PBE) functional.[26,27] The GGA take uneven distribution of the electron into account, making the results of the calculated values are more accurate.[28] In order to better understand van der Waals, the DFT-D3 method in Grimme is applied to the calculation.[29] At the same time, we also carry out adsorption energy correction

[a]*Guangdong Ocean University, Zhanjiang 524088, China. E-mail: njpjh@sina.com*
[b]*Institute of Microscale Optoelectronics, Shenzhen University, Shenzhen 518060, China. E-mail: weisongrui@126.com*
[c]*National Supercomputing Center in Shenzhen (Shenzhen Cloud Computing Center), Shenzhen 518055, China*

about zero point vibrational energy. In order to evaluate the adsorption capacity of PbSe nanoplates to SO_2 and Cl_2, we use a single layer PbSe with a vacuum layer thickness of 30 Å and a multi-layer PbSe structure with a vacuum layer thickness of 40 Å. During structure optimization and electronic self-consistent calculation, a plane wave cut-off of 500 eV and a *k*-point mesh of 3 × 3 × 1 in the Gamma sampling scheme are used. The EDIFFG of structure optimization is 10^{-5} eV, and the EDIFFG of electronic self-consistent is 10^{-7} eV. Also, we select three high symmetry points: *Γ*, *M* and *K*, and twenty *k* points are taken between every two highly symmetrical points in the band calculation. The cut-off energy of 500 eV is also adopted throughout the band calculation, until the threshold of 10^{-7} eV is reached. The single layer and multi-layer structures of 2D PbSe are shown in Fig. 1. The single layer PbSe has a rocksalt crystal structure, and Delerue C. has reported the synthesis and microstructure of this material.[21]

The adsorption energy is obtained from the following formula:

$$E = E_{\text{total}} - E_{\text{PbSe}} - E_{\text{gas}} \quad (1)$$

where E_{total} is the energy of PbSe nanochips with SO_2 or Cl_2 gas, E_{PbSe} is the energy of 2D PbSe nanochips, and E_{gas} is the energy of a single SO_2 or Cl_2 gas molecule. Vaspkit package is used for post-processing of VASP calculation,[30] which includes *k* point path generation, band gap calculating, Bader charge calculation and differential charge density diagram.

3. Results and discussion

First of all, we calculate the adsorption energy of SO_2 and Cl_2 on single layer PbSe. The results are shown in Table 1. In this table, $PbSeSO_2$ is the adsorption system of SO_2 and single layer PbSe. $PbSeCl_2$ is the adsorption system of Cl_2 and single layer PbSe. It is found that the adsorption energy of SO_2 and Cl_2 are both negative. So, SO_2 and Cl_2 molecular can be easily adsorbed on single layer PbSe. It is the basis for sensor applications.

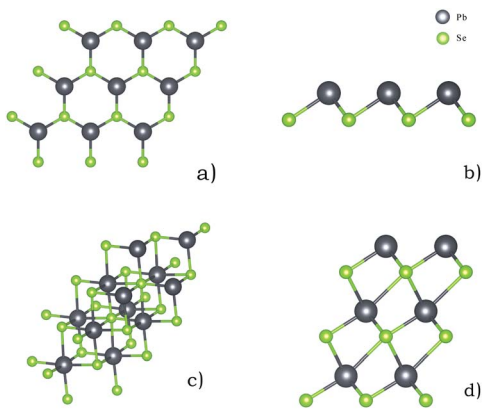

Fig. 1 Single layer PbSe and multi-layer PbSe structure ((a) is single layer PbSe, and (b) is a side view of it; (c) is multi-layer PbSe, and (d) is a side view of it).

Table 1 Adsorption energy of single layer PbSe for SO_2 and Cl_2

Material	Cl_2	PbSe	$PbSeCl_2$	Adsorption energy
Energy (eV)	−3.73	−72.95	−79.38	−2.70
Material	SO_2	PbSe	$PbSeSO_2$	Adsorption energy
Energy (eV)	−17.22	−72.95	−90.50	−0.33

At the same time, we also consider the effect of van der Waals (vdW) on the adsorption energy. The results are shown in Table 2. According to the analysis, we can find that without considering the influence of vdW, the adsorption energy of single layer PbSe for both gases is positive. On the contrary, after considering the influence of vdW, the adsorption energy of single layer PbSe for both gases is negative. Therefore, the vdW plays an important role in the adsorption of single layer PbSe to Cl_2 and SO_2.

We find that the bond length of Cl–Cl changed greatly, the bond length before adsorption is 1.99 Å, the bond length after adsorption is 6.14 Å. So, we can draw a conclusion that chemisorption occurs simultaneously when PbSe adsorbs Cl_2. The larger adsorption energy in Table 1 also proves this situation. However, we didn't find this situation before and after PbSe adsorbs SO_2.

As for adsorption sites, we explore the adsorption of gas on both sides of 2D materials. It is found that the Se atom side cannot adsorb SO_2 and Cl_2 while the Pb atom side can adsorb SO_2 and Cl_2.

Traditional, conductivity is usually used as indicator of many sensors. If the change of conductivity is larger before and after the adsorption, the sensor is more sensitive. As the conductivity is related with the size of band gap, we calculate the band gap before and after the adsorption. The results of single layer PbSe are shown in Fig. 2. The band gap of PbSe, $PbSeCl_2$ and $PbSeSO_2$ are 1.98 eV, 0.78 eV and 1.15 eV, respectively. From these data, we can find that with the adsorption of SO_2 and Cl_2, the band gap of the material decreases obviously, it means that the conductivity of the material is significantly enhanced,[31–33] the smaller band gap after Cl_2 is adsorbed corresponds to the smaller PbSe resistance caused by Cl doping in Wang's report.

Table 2 Adsorption energy of single layer PbSe for SO_2 and Cl_2 (without vdW)

Material	Cl_2	PbSe	$PbSeCl_2$	Adsorption energy
Energy (eV)	−3.73	−72.95	−76.10	0.58
Material	SO_2	PbSe	$PbSeSO_2$	Adsorption energy
Energy (eV)	−17.22	−72.95	−86.56	3.61

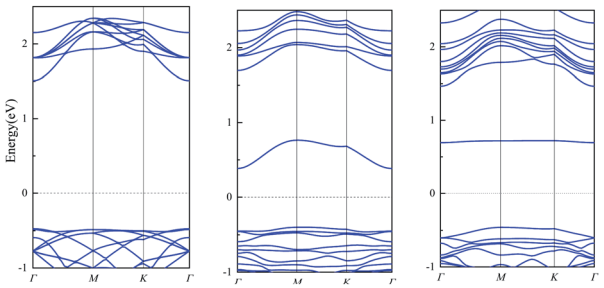

Fig. 2 The band diagram before and after adsorption ((left) shows the energy band diagram of single layer PbSe, (mid) shows the energy band diagram of $PbSeCl_2$ adsorption system, and (right) shows the energy band diagram of $PbSeSO_2$ adsorption system).

Table 3 Changes of electron gain and loss of atoms before and after adsorption of SO_2 and Cl_2 by single layer PbSe

Atom	Before adsorption (e)	After adsorption (e)	Gain (+) and loss (−) electron (e)
Cl	6.994	7.665	+0.671
Cl	6.995	7.591	+0.596
S	3.694	4.000	+0.306
O	7.144	7.205	+0.061
O	7.144	7.203	+0.059

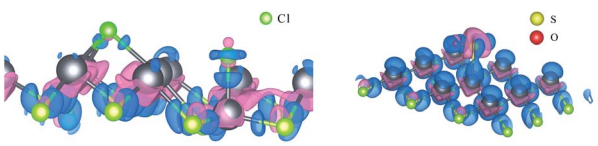

Fig. 3 Differential charge density diagram after single layer PbSe adsorption ((left) shows $PbSeCl_2$ adsorption system and (right) shows $PbSeSO_2$ adsorption system).

Table 4 Adsorption energy of multi-layer PbSe for SO_2 and Cl_2

Material	Cl_2	muPbSe	$muPbSeCl_2$	Adsorption energy
Energy (eV)	−3.73	−100.76	−108.57	−4.08
Material	SO_2	muPbSe	$muPbSeSO_2$	Adsorption energy
Energy (eV)	−17.22	−100.76	−119.02	−1.03

So, conductivity is a sensitive indicator for detecting SO_2 and Cl_2 for single layer PbSe.

The selection specificity of sensors is also investigated. In order to ensure that the sensor is not affected by other gases in the air, we calculate the adsorption of N_2 and O_2, they account for the largest proportion in the air. The adsorption energies of N_2 and O_2 are positive. So, N_2 and O_2 cannot adsorb on 2D PbSe and it will not cause significant changes in conductivity due to the presence of O_2 and N_2 in the air.

Table 5 Adsorption energy of multi-layer PbSe for SO_2 and Cl_2 (without vdW)

Material	Cl_2	muPbSe	$muPbSeCl_2$	Adsorption energy
Energy (eV)	−3.73	−100.76	−101.31	3.18
Material	SO_2	muPbSe	$muPbSeSO_2$	Adsorption energy
Energy (eV)	−17.22	−100.76	−111.74	6.24

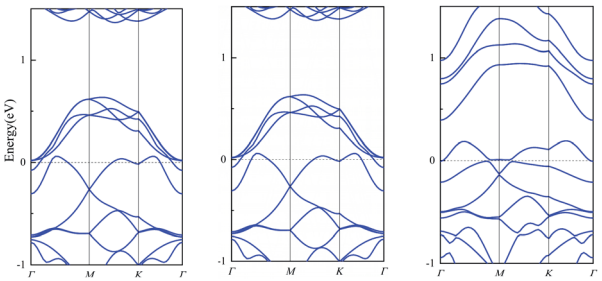

Fig. 4 The band diagram before and after adsorption ((left) shows the band diagram of muPbSe, (mid) shows the band diagram of $muPbSeCl_2$ adsorption system, and (right) shows the band diagram of $muPbSeSO_2$ adsorption system).

Table 6 Changes of electron gain and loss of atoms before and after adsorption of SO_2 and Cl_2 by multi-layer PbSe

Atom	Before adsorption (e)	After adsorption (e)	Gain (+) and loss (−) electron (e)
Cl	6.994	7.628	+0.634
Cl	6.995	7.623	+0.628
S	3.694	4.442	+0.748
O	7.144	7.198	+0.054
O	7.144	7.199	+0.055

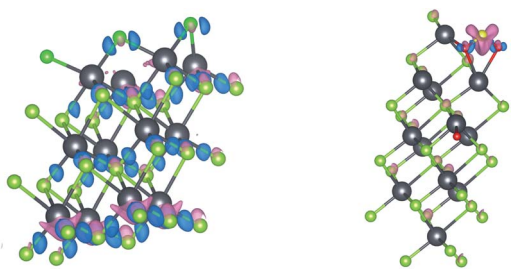

Fig. 5 Differential charge density diagram after muPbSe adsorption ((left) shows $muPbSeCl_2$ adsorption system and (right) shows $muPbSeSO_2$ adsorption system).

In order to further explore the adsorption of SO_2 and Cl_2 on PbSe, we study the electron transfer. We calculate the differential charge density and the Bader charge.[34,35] The details are shown in Table 3 and Fig. 3. For Fig. 3, the blue part is the

electron loss area and the purple part is the electron gain area. We can see that the Cl–Cl bond between Cl atoms breaks after the Cl_2 is absorbed by PbSe, while the chemical bond in SO_2 of S atom and O atom in Bader charge calculation. We can conclude that the adsorption of monolayer PbSe to Cl_2 is chemical adsorption, and the adsorption of monolayer PbSe to SO_2 is physical adsorption.

From the differential charge density diagram, it is found that the charge density of Pb atoms near the adsorption gas changes significantly, and the electrons have been transferred from the Pb atoms, resulting in changes in the electron densities around Cl and S atoms. Therefore, we can conclude that the interaction between the single layer PbSe and the adsorption gas changes the electronic structure of both the 2D material and gas molecular and the electronic transport property of the single layer PbSe.

For Table 3, we can see that all gas atoms get electrons. Among them, Cl atoms get the most electrons, while O atoms get almost no electrons, but the S atom get some electrons. So, the S atom must have got some electrons from PbSe. Fig. 3 proves this, the Pb atom near the S atom transfers some electrons to the S atom.

Meanwhile, we also explore the multi-layer PbSe (muPbSe). It consists three single layers of PbSe. The adsorption energies of SO_2 and Cl_2 on muPbSe are calculated. The results are shown in Table 4, where $muPbSeSO_2$ is the adsorption system of SO_2 and multi-layer PbSe, and $muPbSeCl_2$ is the adsorption system of Cl_2 and multi-layer PbSe. It is found that SO_2 and Cl_2 can also be adsorbed on muPbSe.

At the same time, we also consider the effect of vdW on the adsorption energy. The results are shown in Table 5. According to the analysis, we can find that without considering the influence of vdW, the adsorption energy of multi-layer PbSe for both gases is positive. On the contrary, after considering the influence of vdW, the adsorption energy of multi-layer PbSe for both gases is negative. Therefore, the vdW plays an important role in the adsorption of multi-layer PbSe to Cl_2 and SO_2.

We also find that the bond length of Cl–Cl changed greatly, the bond length after adsorption is 4.25 Å. So, we can draw a conclusion that chemisorption occurs simultaneously when muPbSe adsorbs Cl_2. The larger adsorption energy in Table 4 also proves this situation. However, we didn't find this situation before and after muPbSe adsorbs SO_2. Because of the chemisorption, Cl atoms are difficult to desorb from materials, PbSe can only be used as disposable gas detection material when used to detect Cl_2.

The band structures of muPbSe, $muPbSeSO_2$ and $muPbSeCl_2$ are shown in Fig. 4. The band gap of muPbSe, $muPbSeCl_2$ and $muPbSeSO_2$ are 0.74 eV, 0.42 eV and 0.20 eV, respectively. The band gap decreases when PbSe changes from single layer to three layers, which is consistent with Li's research.[36] Thus, multi-layer PbSe can still be used as gas sensor for Cl_2 and SO_2. At the same time, by analyzing the changes in the band gap between multi-layer PbSe and single layer PbSe before and after adsorption, it can be found that the band gap of multi-layer PbSe decrease by 72.97% before and after SO_2 adsorption, the band gap of multi-layer PbSe decrease by 43.24% before and after Cl_2 adsorption. The band gap of single layer PbSe decrease by 41.92% before and after SO_2 adsorption, the band gap of single layer PbSe decrease by 60.61% before and after Cl_2 adsorption. So, we can draw a conclusion that single layer PbSe is more sensitive to Cl_2 and multi-layer PbSe is more sensitive to SO_2.

The Bader charge of muPbSe is shown in Table 6. It can be seen that there is charge transfer between the gas and the 2D material. The situation is similar to that of single-layer PbSe adsorption SO_2 and Cl_2. Cl atoms still get more electrons, and we can compare the situation with adsorption energy, larger adsorption energy corresponds to more electron transfer. And Pb atoms near adsorbed gas molecules still provide the most electrons.

The differential charge density is shown in Fig. 5. It can be seen that the electrons transfer between multi-layer PbSe and adsorbed gas, it changes the electronic structure around multi-layer PbSe and adsorbed gas. It is found that the bond between Cl atoms breaks, while the chemical bond in SO_2 does not break. The adsorption of SO_2 on multi-layer PbSe is physical adsorption while adsorption of Cl_2 on multi-layer PbSe is chemical adsorption. The electron transfer of SO_2 and Cl_2 on multi-layer PbSe in the differential charge density is consistent with the Bader charge calculation results. Therefore, we can conclude that the interaction between multi-layer PbSe and adsorbed gas changes the electronic structure of both the multi-layer PbSe and gas molecular and the electronic transport property of multi-layer PbSe.

4. Conclusions

In conclusion, based on first principle calculation, we have proved that the PbSe nanosheet can be a potential material for the SO_2 and Cl_2 monitoring and sensing system. We obtain the following results: SO_2 and Cl_2 can be adsorbed on the Pb atom side of single layer PbSe and multi-layer PbSe materials, but not on the Se atom side. After single layer PbSe and multi-layer PbSe adsorb Cl_2, the bond between Cl atoms breaks, it is chemisorption. When SO_2 is adsorbed, the bond does not break, it is physical adsorption. The band gap of single layer PbSe and multi-layer PbSe are significantly smaller after adsorption SO_2 and Cl_2, indicating that 2D PbSe is suitable for monitoring SO_2 and Cl_2. PbSe can only be used as disposable gas detection material when used to detect Cl_2, PbSe can be recycled as gas detection material when used to detect SO_2. Single layer PbSe is more sensitive to Cl_2 and multi-layer PbSe is more sensitive to SO_2. There is charge transfer between PbSe and SO_2, Cl_2 before and after the adsorption. In summary, 2D PbSe is a potential possibility material to design gas sensors for monitoring SO_2 and Cl_2.

Conflicts of interest

There are no conflicts to declare.

Acknowledgements

This research was funded by National Natural Science Foundation of China, grant number 51709150 and Special Project of

Guangdong Province to promote high-quality economic development, grant number GDNRC[2021]56.

Notes and references

1 M. Naguib, V. N. Mochalin, M. W. Barsoum and Y. GogotsiMXenes, A New Family of Two-dimensional Materials, *Adv. Mater.*, 2013, **26**, 992–1005.

2 N. R. Glavin, R. Rao, V. Varshney, E. Bianco, A. Apt, A. Roy, E. Ring and P. M. Ajayan, Emerging Applications of Elemental 2D Materials, *Adv. Mater.*, 2020, **32**, 1904302.

3 K. Leng, W. Fu, Y.-P. Liu, M. Chhowalla and K. P. Loh, From Bulk to Molecularly Thin Hybrid Perovskites, *Nat. Rev. Mater.*, 2020, **5**, 482–500.

4 C. Liu, L. Wang, J.-J. Qi and K.-H. Liu, Designed Growth of Large-Size 2D Single Crystals, *Adv. Mater.*, 2020, **32**, 2000046, DOI: 10.1002/adma.202000046.

5 Y.-Z. Zhang, Y. Wang, Q. Jiang, J. K. El-Demellawi, H. Kim and H. N. Alshareef, MXene Printing and Patterned Coating for Device Applications, *Adv. Mater.*, 2020, **32**, 1908486, DOI: 10.1002/adma.201908486.

6 Y. Gogotsi and B. Anasori, The Rise of MXenes, *ACS Nano*, 2019, **13**, 8491–8494.

7 A. A. A. Jafry, A. R. Muhammad, N. Kasim, A. H. A. Rosol and P. Yupapin, Ultrashort Pulse Generation with MXene $Ti_3C_2T_x$ Embedded in PVA and Deposited onto D-shaped Fiber, *Opt. Laser Technol.*, 2021, **136**, 106780, DOI: 10.1016/j.optlastec.2020.106780.

8 D. K. Sang, H.-D. Wang, Z.-N. Guo, N. Xie and H. Zhang, Recent Developments in Stability and Passivation Techniques of Phosphorene toward Next-Generation Device Applications, *Adv. Funct. Mater.*, 2019, **29**, 1903419, DOI: 10.1002/adfm.201903419.

9 S.-Y. Guo, Y.-P. Zhang, Y.-Q. Ge, S.-L. Zhang, H.-B. Zeng and H. Zhang, 2D V-V Binary Materials: Status and Challenges, *Adv. Mater.*, 2019, **31**, 1902352, DOI: 10.1002/adma.201902352.

10 G. Cheng and C. Zhang, Desulfurization and Denitrification Technologies of Coal-fired Flue Gas, *Pol. J. Environ. Stud.*, 2018, **27**, 481–489.

11 Q. Xu, C. Lu, R. G. Murithi and L. Cao, Increase Associated Risk of Gynaecological Cancer Due to Long-term Exposure to High Concentration of Atmospheric SO_2 Industrial Pollutant, *Indoor Built Environ.*, 2021, 1420326X211003655.

12 Y.-J. Su, J.-J. Wang, B. Wang, T.-N. Yang, B.-X. Yang, G.-Z. Xie, Y.-H. Zhou, S.-L. Zhang, H.-L. Tai, Z.-X. Cai, G.-R. Chen, Y. D. Jiang, L. Q. Chen and J. Chen, Alveolus-inspired Active Membrane Sensors for Self-powered Wearable Chemical Sensing and Breath Analysis, *ACS Nano*, 2020, **14**, 6067–6075.

13 D.-W. Ma, J. Zhang, X.-X. Li, C.-Z. He, Z.-W. Lu, Z.-S. Lu, Z.-X. Yang and Y.-X. Wang, C_3N Monolayers as Promising Candidates for NO_2 Sensors, *Sens. Actuators, B*, 2018, **266**, 664–673.

14 T. Nakotte, H. Luo and J. Pietryga, PbE (E = S, Se) Colloidal Quantum Dot-Layered 2D Material Hybrid Photodetectors, *Nanomaterials*, 2020, **10**, 172.

15 I. Skurlov, A. Sokolova, T. Galle, S. Cherevkov, E. Ushakova, A. Baranov, V. Lesnyak, A. Fedorov and A. Litvin, Temperature-Dependent Photoluminescent Properties of PbSe Nanoplatelets, *Nanomaterials*, 2020, **10**, 2570, DOI: 10.3390/nano10122570.

16 B. U. Haq, S. Alfaify, R. Ahmed, A. Laref and E. Algrafy, Optoelectronic Properties of PbSe Monolayers from First-principles, *Appl. Surf. Sci.*, 2020, **525**, 146521, DOI: 10.1016/j.apsusc.2020.146521.

17 S. V. Ovsyannikov, V. V. Shchennikov, S. V. Popova and A. Y. Derevskov, Semiconductor-metal Transitions in Lead Chalcogenides at High Pressure, *Phys. Status Solidi B*, 2003, **235**, 521–525.

18 S. V. Ovsyannikov, V. V. Shchennikov, A. Y. Manakov, A. Y. Likhacheva, Y. S. Ponosov, V. E. Mogilenskikh, A. P. Vokhmyanin, A. I. Ancharov and E. P. Skipetrov, Unusual B1-B2 Transition in PbSe Under High Pressure: Evidence for Two Intermediate Phases; Transport, Structural, and Optical Properties, *Phys. Status Solidi B*, 2009, **246**, 615–621.

19 V. V. Shchennikov, S. V. Ovsyannikov and A. Y. Derevskov, Thermopower of Lead Chalcogenides at High Pressures, *Phys. Solid State*, 2002, **44**, 1845–1849.

20 S.-M. Wang, C.-P. Zang, Y.-K. Wang, L.-P. Wang, J.-Z. Zhang, C. Childs, H. Ge, H.-W. Xu, H.-Y. Chen, D.-W. He and Y.-S. Zhao, Revisit of Pressure-Induced Phase Transition in PbSe: Crystal Structure, and Thermoelastic and Electrical Properties, *Inorg. Chem.*, 2015, **54**, 4981–4989.

21 C. Delerue and D. Vanmaekelbergh, Electronic Band Structure of Zinc Blende CdSe and Rock Salt PbSe Semiconductors with Silicene-type Honeycomb Geometry, *2D Mater.*, 2015, **2**, 034008, DOI: 10.1088/2053-1583/2/3/034008.

22 H. Wang, M. I. Fedorov, A. A. Shabaldin, P. P. Konstantinov and G. J. Snyder, Comparison of Thermoelectric Transport Measurement Techniques Using n-type PbSe, *J. Electron. Mater.*, 2015, **44**, 1967–1971.

23 G. Kresse and J. Hafner, Ab initio Molecular-dynamics Simulation of the Liquid-metal–amorphous-semiconductor Transition in Germanium, *Phys. Rev. B: Condens. Matter Mater. Phys.*, 1994, **49**, 14251–14269.

24 G. Kresse and J. Furthmüller, Efficiency of ab initio Total Energy Calculations for Metals and Semiconductors Using a Plane-wave Basis Set, *Comput. Mater. Sci.*, 1996, **6**, 15–50.

25 G. Kresse and J. Furthmüller, Efficient Iterative Schemes for ab initio Total-energy Calculations Using a Plane-wave Basis Set, *Phys. Rev. B: Condens. Matter Mater. Phys.*, 1996, **54**, 11169–11186.

26 P. E. Blochl, Projector Augmented-wave Method, *Phys. Rev. B: Condens. Matter Mater. Phys.*, 1994, **50**, 17953–17979.

27 J. P. Perdew, K. Burke and M. Ernzerhof, Generalized Gradient Approximation Made Simple, *Phys. Rev. Lett.*, 1996, **77**, 3865–3868.

28 S.-Y. Xia, L.-Q. Tao, T.-Y. Jiang, H. Sun and J. Li, Rh-doped h-BN Monolayer as a High Sensitivity SF_6 Decomposed Gases Sensor: A DFT Study, *Appl. Surf. Sci.*, 2021, **536**, 147965, DOI: 10.1016/j.apsusc.2020.147965.

29 S. Grimme, Semiempirical GGA-type density functional constructed with a long-range dispersion correction, *J. Comput. Chem.*, 2006, **27**, 1787–1799.
30 V. Wang, N. Xu, J.-C. Liu, G. Tang and W.-T. Geng, VASPKIT: A user-friendly interface facilitating high-throughput computing and analysis using VASP code, *Comput. Phys. Commun.*, 2021, 108033, DOI: 10.1016/j.cpc.2021.108033.
31 H. Cui, X.-X. Zhang, D.-C. Chen and J. Tang, Pt & Pd Decorated CNT as a Workable Media for SOF_2 Sensing: A DFT study, *Appl. Surf. Sci.*, 2018, **471**, 335–341.
32 H. Cui, X.-X. Zhang, G.-Z. Zhang and J. Tang, Pd-doped MoS_2 Monolayer: A Promising Candidate for DGA in Transformer Oil Based on DFT Method, *Appl. Surf. Sci.*, 2019, **470**, 1035–1042.
33 H. Cui, X.-X. Zhang, Y. Li, D.-C. Chen and Y. Zhang, First-principles Insight into Ni-doped InN Monolayer as a Noxious Gases Scavenger, *Appl. Surf. Sci.*, 2019, **494**, 859–866.
34 M. Yu and D. R. Trinkle, Accurate and Efficient Algorithm for Bader Charge Integration, *J. Chem. Phys.*, 2011, **134**, 064111, DOI: 10.1063/1.3553716.
35 W. Tang, E. Sanville and G. Henkelman, A Grid-based Bader Analysis Algorithm Without Lattice Bias, *J. Phys.: Condens. Matter*, 2009, **21**, 084204, DOI: 10.1088/0953-8984/21/8/084204.
36 X.-B. Li, P. Guo, Y.-N. Zhang, R.-F. Peng, H. Zhang and L.-M. Liu, High carrier mobility of few-layer PbX (X = S, Se, Te), *J. Mater. Chem. C*, 2015, **3**, 6284–6290.